JOURNAL OF SOLID STATE CHEMISTRY 27, 287–292 (1979)

Fluorite-related Phases Ln_3MO_7, Ln = Rare-earth, Y or Sc, M = Nb, Sb or Ta
III. Structure of the Non-stoichiometric Y_3TaO_7 Phase

H. J. ROSSELL

CSIRO, Division of Materials Science, Engineering Ceramics and Refractories Laboratory, P.O. Box 4331, GPO, Melbourne 3001, Victoria, Australia

Received March 11, 1978

The orthorhombic fluorite-related superstructure phase Y_3TaO_7 is non-stoichiometric; the Y_2O_3 content may be varied from 75.0 to about 72.5 mole% without incurring structural changes. For overall Y_2O_3 contents from 72.0 to 70.5 mole%, the crystal symmetry changes from $C222_1$ to $Cmmm$, and the c axis becomes halved. The structure of the low-Y_2O_3 material has been determined from powder X-ray diffraction intensities supplemented by single crystal electron-optical data. The relationship of this structure to that of stoichiometric Y_3TaO_7 is discussed.

Introduction

The orthorhombic fluorite-related superstructure phases Ln_3MO_7, Ln = rare-earth, Y or Sc, M = Nb, Ta or Sb, have been described in Parts I and II of this work (*1*) (*2*). In Part I, it was reported that several of these phases exhibit an apparent range of stoichiometry, and that this was widest for the Y_3TaO_7 and Ho_3TaO_7 phases. The Y_3TaO_7 phase was selected for more detailed study, mainly because of the relatively large difference in X-ray scattering factors of Y and Ta.

Lattice parameters of the Y_3TaO_7 phase in specimens of various composition have been determined. The results show that the apparent extent of the homogeneity range at 1370°C is from 70.5 to 75.0 mole% Y_2O_3: The lattice parameters of the Y_3TaO_7-type unit cell vary smoothly over this composition range, while specimens of composition 70.0 and 75.9 mole% Y_2O_3 are two-phase, and contain small amounts of the $YTaO_4$ fergusonite phase and of a defect fluorite-type phase respectively. A report of the phase relationships in the system Y_2O_3–Ta_2O_5 will be published elsewhere. The present paper is concerned with structural changes that occur in the Y_3TaO_7 phase over its composition range.

Experimental

Starting materials and preparation techniques were as described in Part I. Y_2O_3–Ta_2O_5 specimens of composition 70.0, 70.7, 71.4, 72.0, 72.5, 73.0, 73.5, 74.0, 74.5, 75.0 and 75.9 mole% Y_2O_3 were prepared by sintering compacts of the mixed component oxide powders at 1370°C for periods from 10 to 150 days. The phases formed were largely independent of the sintering time: However, specimen crystallinity slowly improved as sintering time increased. Significantly higher sintering temperatures could not be used since the phase disorders to a defect fluorite-type structure above 1500°C.

The techniques for electron diffraction and microscopy, and those for collection and processing of X-ray powder diffraction

0022-4596/79/030287-06$02.00/0

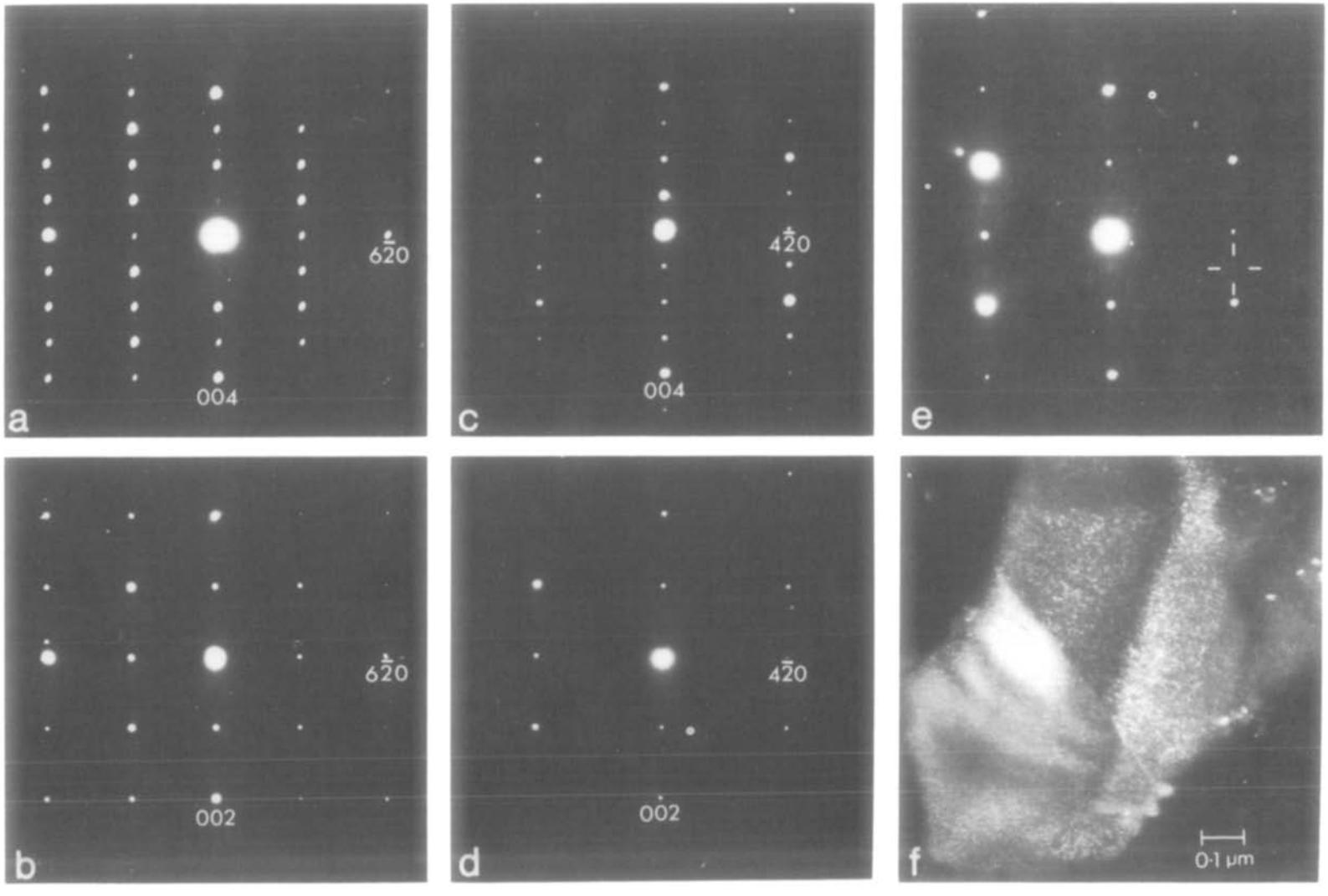
a
004
$6\bar{2}0$
b
002
$6\bar{2}0$
c
004
$4\bar{2}0$
d
002
$4\bar{2}0$
e
f
0·1 μm

intensities for structure refinement were those described in Parts I and II respectively.

Results

1. Electron-optical Studies.

Electron diffraction patterns from the various specimens showed that the structure of the Y_3TaO_7 phase was different at the extremes of its apparent homogeneity range.

For specimens with a Y_2O_3 content greater than about 73 mole%, patterns typical of Y_3TaO_7 itself were observed. As shown in Parts I and II, Y_3TaO_7 is a fluorite-related superstructure phase, space group $C222_1$, the unit cell of which has axes related by the matrix $200/011/0\bar{1}1$ to those of the fluorite subcell.

Specimens with compositions below 72 mole% Y_2O_3, however, gave somewhat different electron diffraction patterns, some examples of which are shown in Fig. 1. Strong reflections typical of a fluorite-type subcell are present, as in Y_3TaO_7, but superlattice reflections *hkl* with *l* odd (Y_3TaO_7-type indexing) are absent. Thus, the *c* axis of the superstructure has become halved relative to that of stoichiometric Y_3TaO_7, and the supercell axes are now $200/011/0\frac{\bar{1}1}{22}$ in terms of the subcell axes.

This change in the *c* dimension could not be discerned readily from the Guinier photographs of the specimens. Reflections *hkl* with *l* odd, which are all weak supercell reflections in stoichiometric Y_3TaO_7, became weaker as the Y_2O_3 content was lowered, until in specimens of about 72.5 mole% Y_2O_3, they were faintly visible only after massive exposures. Moreover, if the Guinier patterns of all specimens were indexed on the basis of the unit cell appropriate to stoichiometric Y_3TaO_7, the derived lattice parameters varied smoothly with composition over the range 70.5–75.0 mole% Y_2O_3, as normally would be expected for single phase material.

For some specimens with compositions near 72 mole% Y_2O_3, single crystal electron diffraction patterns were recorded which were of the Y_3TaO_7 type, but which had *diffuse* reflections *hkl* for *l* odd (Fig. 1e). In some instances, dark field images formed with such diffuse reflections showed that they arose from discrete regions in the crystal of about 70A diameter (Fig. 1f): In other cases, no such detail could be seen.

Since stringent crystal selection criteria apply in the electron microscopy of a sample, it was impossible to see if all crystals in a specimen gave these diffuse reflections. For the same reason, the composition range of the specimens showing this effect could not be determined, and nor could it be ascertained if the effect was correlated with sintering time.

An examination of the non-stoichiometric Ho_3TaO_7 phase showed that a structure change, similar to that described above, occurred at the low-Ho_2O_3 end of the apparent composition range (~72 mole%).

2. Structure Determination of the low-Y_2O_3 Orthorhombic Phase

The only condition limiting reflections in the electron diffraction patterns of the new structure is $h + k \neq 2n$ for all *hkl*. The space group is therefore one of *Cmmm* (No. 65, D_{2h}^{19}), *Cm2m* or *C2mm* (alternative settings of *Amm2*, No. 38, C_{2v}^{14}), *Cmm2* (No. 35, C_{2v}^{11}) or *C222* (No. 21, D_2^6). The unit

FIG. 1. Electron diffraction patterns typical of the Y_3TaO_7 phase near the extremes of its homogeneity range. Reflection indices refer to the supercell. (a) Stoichiometric Y_3TaO_7 in the [233] subcell orientation. (b) Ta_2O_5—71.4 mole% Y_2O_3, also in the [233] subcell orientation. The *c* axis of the supercell has become halved. (c), (d) Specimens of the same composition as those in (a) and (b) respectively, but with subcell orientation [111]. (e) A different specimen of Ta_2O_5—71.4 mole% Y_2O_3, [111] subcell orientation. (f) Dark field image of the specimen in (e), formed with the indicated diffuse reflection.

cell ideally contains two M_4O_8 fluorite subunits.

X-ray powder diffraction intensity data were collected with Cu Kα radiation from specimens of composition 70.7 and 71.4 mole% Y_2O_3, for reflections with $2\theta \leq 90°$. For these specimens, the unit cell contents are $Y_{5.656}Ta_{2.344}O_{14.344}V_{1.656}$ and $Y_{5.712}Ta_{2.288}O_{14.288}V_{1.712}$ respectively (V = oxygen vacancy), assuming an intact cation sublattice exists, in common with all known fluorite-related superstructures. Densities calculated on this basis, $6.68\ g \cdot cm^{-3}$ (70.7 mole% Y_2O_3) and $6.64\ g \cdot cm^{-3}$ are in fair agreement with the pycnometric densities of $6.5 \pm 0.1\ g \cdot cm^{-3}$.

The structure was determined by a trial and error procedure similar to that outlined in Part II. The atoms were initially assumed to be in ideal fluorite-derived positions, with the cations randomly distributed and all anion sites occupied. Structure refinement was attempted in all of the possible space groups. Degeneracy in the starting model was removed by preliminary shifts in some atomic parameters, and all variations in the senses of these shifts were tried. Models were retained or rejected according to the resultant value of the residual R.

The distribution of Y and Ta was assessed through refinement of the cation site occupancies. This showed that only one of the relevant sets of positions was occupied by both Y and Ta, and so the final distribution was chosen to satisfy the known composition. A similar situation occurred for the anion distribution.

An overall isotropic temperature factor of zero was used: If refined, the value remained close to this, with a relatively large calculated standard deviation.

The refinement procedure in *Cmmm* yielded only one structure with an acceptable residual: The parameters for this structure are given in Table I. Refinement in the other, i.e. the acentric, space groups yielded essentially the same structure, but gave no significant improvement in the fit of observed and calculated intensities, despite the greater number of variable parameters.

Discussion

The Ta_2O_5—70.7 and 71.4 mole% Y_2O_3 materials have the same structure, which, despite the symmetry difference, is essentially that of Y_3TaO_7 with a few minor alterations.

In Y_3TaO_7, there are slabs parallel to (100), which are composed of alternate [001] rows of TaO_6 octahedra and YO_8 cubes containing one third of the Y atoms. Such slabs alternate with sheets of the remaining Y atoms in sevenfold coordination by O (Part II). The TaO_6 octahedra are corner linked through the oxygen atom designated O III. Successive O III atoms along a [001] row lie in the zig-zag sequence $(-x, 0, 0)$, $(x, 0, \frac{1}{2}), \ldots$, with $x \approx \frac{1}{8}$, giving rise to a corresponding sequence of tilts to the octahedra, and compared to the parent fluorite structure, there are formal anion vacancies associated in pairs with each Ta atom in the complementary zig-zag sequence $(\frac{1}{8}, 0, 0)$, $(-\frac{1}{8}, 0, \frac{1}{2}), \ldots$.

The new structure can be envisaged as derived from that of stoichiometric Y_3TaO_7 through the partial substitution of Y by Ta and the filling of vacant anion sites. Substitution of Y by Ta takes place randomly in the interslab 7-coordinated Y sites, but not in the YO_8 cube sites, as may be expected from the smaller cationic radius of Ta^V and its crystal chemistry. The extra oxygen atom introduced with each substituting Ta cation does not occupy randomly a vacant anion site, but rather both the former O III site at $(\sim\frac{1}{8}, 0, 0)$ and the associated vacant site at $(-\frac{1}{8}, 0, 0)$ become equally but partially populated by O on the average, so that compared with Y_3TaO_7, the [001] sequences of alternately tilted TaO_6 octahedra are destroyed.

These partially occupied anion sites coordinated to Ta have a separation of only

TABLE I

CRYSTAL DATA FOR THE PHASES
Ta_2O_5–70.7 MOLE% Y_2O_3 AND Ta_2O_5–71.4 MOLE% Y_2O_3

Numbers in parentheses are calculated standard deviations, which apply to the last quoted places.
Space group: Cmmm (No. 65, D_{2h}^{19}).
Axial relationship to fluorite subcell: $200/011/0\bar{1}1_{22}$.

Ta_2O_5–70.7 mole% Y_2O_3					Ta_2O_5–71.4 mole% Y_2O_3				
$a = 10.4723(9)$A $b = 7.3876(5)$ $c = 3.7152(3)$					$a = 10.4750(7)$A $b = 7.3910(4)$ $c = 3.7170(3)$				
Atom	point set	x	y	z	Atom	point set	x	y	z
Ta	2*d*	0	0	$\frac{1}{2}$	Ta	2*d*	0	0	$\frac{1}{2}$
Y	2*c*	0	$\frac{1}{2}$	$\frac{1}{2}$	Y	2*c*	0	$\frac{1}{2}$	$\frac{1}{2}$
0.914 Y + 0.086 Ta	4*e*	$\frac{1}{4}$	$\frac{1}{4}$	0	0.929 Y + 0.071 Ta	4*e*	$\frac{1}{4}$	$\frac{1}{4}$	0
O I	8*p*	0.121(5)	0.204(9)	$\frac{1}{2}$	O I	8*p*	0.132(8)	0.209(8)	$\frac{1}{2}$
O II	4*g*	0.154(8)	$\frac{1}{2}$	0	O II	4*g*	0.126(17)	$\frac{1}{2}$	0
0.586 O (O III)	4*g*	0.056(10)	0	0	0.571 O (O III)	4*g*	0.057(14)	0	0
71 observations.[a] $R = 0.0746$					37 observations. $R = 0.0458$.				

[a] In this case, the data peaks were comparatively well resolved, so that many sets of closely overlapping reflections could be separated through the use of a microdensitometer trace of the Guinier photograph, as described in Part II.

1.2 A, whereas the more usual anion separation is ~2.8 A. This may be interpreted in terms of the local conditions of ordering. The increase in oxygen content in the new structure relative to that in stoichiometric Y_3TaO_7 is small, viz. about $\frac{1}{6}$ of an oxygen atom for every O III, so that in any given unit cell of the new structure, there is a high probability that of two closely separated partially occupied O sites, one is in fact occupied and the other vacant. The corresponding sites in the unit cell next to this in the *c* direction are in nearest-neighbour coordination with the same Ta cation, and if only one of these sites is occupied also, it is likely to be in the opposite sense to the first as a result of electrostatic effects, producing a TaO_6 octahedron tilted as in Y_3TaO_7. Such correlated occupancy could be expected to continue for several unit cells, resulting in a short sequence of octahedra with alternate tilts. This constitutes an incipient doubling of the *c* periodicity, for which evidence has been obtained in the form of diffuse reflections in electron diffraction patterns (Fig. 1e), and there is evidence (Fig. 1f) that the correlation can occur over relatively large regions.

A sequence of O III sites occupied in the ordered way proposed above, will be terminated when both members of a close pair are occupied simultaneously, and it is suggested that when this occurs, the anions involved in fact lie further apart, in approximately the ideal fluorite positions $(\frac{1}{8}, 0, 0)$ and $(-\frac{1}{8}, 0, 0)$. The average position determined for O III would include only a small contribution from such atoms, since double occupation is of relatively low frequency. It is suggestive, in this regard, that when

individual isotropic temperature factors for the various atoms were refined, that for O III assumed a value of about 7, while the others remained close to zero, the value of the overall temperature factor. The improvement in the fit of observed and calculated intensities, however, was not significant.

Thus the solid solution of Ta_2O_5 in Y_3TaO_7 is accompanied by a change in crystal symmetry and the production of a defect structure, which can be derived from the Y_3TaO_7 structure by relatively small alterations. The accommodation of the extra oxygen is associated with the presence of sites in Y_3TaO_7, which, compared to the parent fluorite substructure, are the locations of formal anion vacancies. Phases which have the same structure of Y_3TaO_7 exhibit similar homogeneity ranges, and in the case of Ho_3TaO_7 at least, similar composition-dependant structural changes occur also, so that it is tempting to associate the relatively narrow ranges of stoichiometry exhibited by such phases as La_3NbO_7 and Nd_3NbO_7 (Part I) with the absence of formal anion vacancies in their structures.

References

1. J. G. ALLPRESS AND H. J. ROSSELL, *J. Solid State Chem.* **26**, xx (1978).
2. H. J. ROSSELL, *J. Solid State Chem.* **26**, xx (1978).